Wavelet Transform Coherence Estimates in Cardiovascular Analysis: Error Analysis and Feasibility Study

K Keissar, LR Davrath, S Akselrod

The Abramson Center for Medical Physics, Tel Aviv University, Tel Aviv, Israel

Abstract

Wavelet transform coherence (WTC) can provide insight into the transient linear order of the regulatory mechanisms, via the computation of time-frequency maps of the time-variant coherence. This paper presents a framework for applying WTC for quantitative analysis of coherence in cardiovascular variability research. Computer simulations were performed to estimate the accuracy of the WTC estimates and a method for determining the coherence threshold for specific frequency band was developed and evaluated. Finally, we demonstrated, in two representative situations, the dynamic behavior of RSA through the analysis of the WTC between HR and respiration signals. This emphasizes that continuous wavelet transform (CWT) and its application to WTC is a useful tool for dynamic analysis of cardiovascular variability.

1. Introduction

The coherence function is used to assess the existence and strength of linear coupling between two signals in the frequency domain [1]. As such, it is often applied to the analysis of the ANS functionality via the examination of cardiovascular and respiratory interrelation [2]. A major limitation of the classical spectral analysis is the steady state assumption. This stipulation makes the selection of suitable segments of the time series quite difficult and makes these methods unsuitable for the analysis of transient phenomena. The use of wavelet transform in bivariate analysis of cardiovascular signals has the potential to offer additional information about the complex functioning of autonomic regulatory mechanisms. The wavelet transform coherence (WTC) is a known, though infrequently used tool in scientific areas. The use of WTC in cardiovascular variability research has already been introduced [3] and further explored [4;5], focusing on the dynamic analysis of RSA. The purpose of the following work is to establish the Wavelet coherence estimates for the use of physiological research, particularly for use in the analysis of ANS control.

2. Methods

2.1. Mathematical overview

Wavelet Transform (WT) decomposes a time series signal into a time – scale plane. The continuous wavelet function based on the Morlet wavelet function consists of a plane wave modulated by a Gaussian .

$$\Psi_0(\eta) = \pi^{-\frac{1}{4}} e^{i\omega_0 t/s} e^{-\frac{1}{2}t/s^2} \tag{1}$$

whereas t and s are time and scale. The Morlet coefficient ω_0 shifts the balance between frequency resolution and time resolution. We found that the preferable choice of time and frequency resolution combination for cardio respiratory signals is $6 \leq \omega_0 \leq 30$.

The squared wavelet coherence estimator is defined as the squared absolute value of the smoothed cross wavelet spectrum, normalized by the smoothed wavelet power spectrum of the two signals

$$\hat{C}_n^2(s) = \frac{\left|\left\langle W_n^{xy}(s) \cdot s^{-1} \right\rangle\right|^2}{\left\langle \left|W_n^{xx}(s)\right| \cdot s^{-1} \right\rangle \left\langle \left|W_n^{yy}(s)\right| \cdot s^{-1} \right\rangle} \tag{2}$$

where n is the discrete time index, W_n^{xx} and W_n^{yy} are the wavelet spectral density function, W_n^{yy} is the cross wavelet spectrum, and the $\langle \ \rangle$ brackets indicate a smoothing operator [6] .

A detailed overview of wavelet analysis based on the Morlet wavelet and of WTC was given in a previous work [3] and is based on the work of Torrence & Compo [7].

2.2. Simulations for assessing bias and SD

In order to assess the statistical error of the WTC with regard to the theoretical coherence, computer simulations

were performed. As our principal simulated signal (X(t)), we chose a white noise signal in the 0.18 – 0.4 Hz band to simulate an arbitrary respiration signal.

In accordance with the LTI model with transfer function equal unity [8], the output signal Y(t) signals were obtained by adding uncorrelated white noise to X(t).

The simulations were performed repeatedly with different amplitudes of the added white noise to give N>1000 realizations for each coherence level, in 0.1 steps.

The bias and standard deviation were obtained as

$$bias(k) \cong \left(\frac{1}{N} \sum^{N} C^2(k) \right) - k = \overline{C^2(k)} - k \qquad (3)$$

$$SD(k) \cong \sqrt{ \frac{1}{N-1} \sum^{N} \left(C^2(k) - \overline{C^2(k)} \right)^2 } \qquad (4)$$

where k is the theoretical coherence levels from 0.05 to 0.95 in 0.1 steps, $C^2(k)$ is the WTC level. The procedure was repeated for different wavelet coefficients (ω_0): 6,10,15,20 and 30.

2.3.   WTC threshold and error rates.

Coherence threshold levels depends on the choice of the surrogate signals used and their similarity to the analyzed signals [9]. Therefore, the evaluation of the threshold for the band coherence is performed using signals created in the same way as the simulated signals described above, but with SNR<<1 which generates uncorrelated signal couples. The critical level for calculating the magnitude threshold was set at 95%. The threshold level was analyzed for the HF band (0.18 – 0.4) for ω_0 : 6,10,15,20 and 30.

In order to evaluate the error rates of the threshold level, simulations similar to those performed for evaluating bias were used; realizations of the signals were analyzed with different SNR values to impose the full scale of coherence levels. For each theoretical coherence level, the WTC band coherence values were compared to the zero threshold level. The false negative rate (β) was calculated by assessing the relative number of coherence estimations which resulted in a value lower than the threshold level.

The simulations were performed repeatedly and gave N>1000 realizations for each coherence level, in 0.1 steps. β was assessed for different wavelet coefficients: 6,10,15,20 and 30.

2.4.   Simulations for assessing the detection of coherence discontinuities

In order to evaluate the ability of the WTC to follow transient changes, we created signals with a series of growing uncorrelated epochs to examine the ability of the WTC to detect and present them in an accurate way.

To establish the ability of the WTC to detect coherence discontinuities within the HF band, 200 simulations for each of the different wavelet coefficients were performed. Using the established threshold levels, detection ratio was calculated for each epoch time. For each wavelet coefficient, the minimal epoch time with a lower limit of 95% detection probability with 95% confidence interval was found.

2.5.   Application to real cardio – respiratory data

The application of the WTC was investigated in experimental data obtained from a group of 8 healthy subjects.

We analyzed two different physiological conditions:

(i). Supine rest for 20 min which represents a static situation without external stimulation. (ii). Change Posture (CP) from supine to standing position, which induces a strong response of the autonomic control system.

Analyses were performed using $\omega_0 = 20$ which was chosen based on results in the previous sections.

Results were presented as means ± SD. Significance calculations between different time regions were calculated using the student t-test for two samples. Results were considered significant for p<0.05.

3.   Results

3.1.   Bias and standard deviation

The bias is positive for low coherence levels, decreases almost linearly with increasing coherence and crosses zero for a small negative bias for all cases other than $\omega_0 = 6$ (Figure 1a). SD value increases as coherence level decreases up to a maximum value. After the maximum point the SD declines to a slightly lower value. As in the bias curve, the SD curves of lower coefficients have larger slope and higher maximum value (Figure 1b).

3.2.   Coherence threshold and detection error rate

The coherence threshold was 0.79, 0.64, 0.5, 0.45 and

0.3 with respect to ω_0 of 6, 10, 15, 20 and 30. The threshold level sets the false positive rate to be α=0.05.

False negative error rates (β) are improved for larger ω_0 (Figure 1c). For $\omega_0 = 30$, the error rate remains close to zero for a coherence level of as low as 0.55. Other slopes exhibit the same behavior with lesser performance. For $\omega_0 = 6$, the error rate rises sharply even for higher coherence levels.
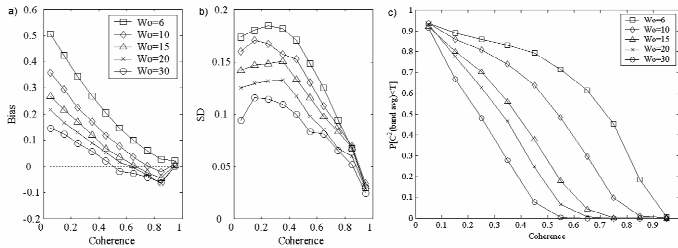

Figure 1 : Band Coherence (a) bias and (b) SD as function of coherence theoretical levels for different wavelet coefficients; (c) Probability estimation of accepting the null hypothesis of coupled signals (false negative rate) for different wavelet coefficients as function of coherence theoretical levels. For HF band averaging.
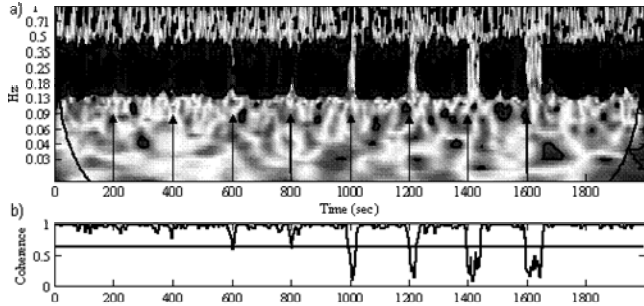

Figure 2: a) Coherence map of simulated coupled signals, for $\omega_0 = 10$. Signals with "uncorrelated" epochs showing discontinuities in the predicted time epochs (arrows showing beginning of each epoch). b) HF band coherence as function of time of power map (a), the horizontal line represents the band threshold showing detection of epoch above 5 sec. The uncorrelated epochs grow from left to right with the following spans: 1, 2, 5, 10, 20, 30, 40, 50 seconds

3.3. Detection of coherence discontinuities

Figure 2a shows coherence map of two signals with "uncorrelated" epochs. The Coherence band in the respiratory frequencies has visible discontinuities whenever there is no correlation between the two signals,

except for the first 1 and 2 second epochs. Time dependent HF band coherence with its appropriate threshold, indicates for this specific example a detection of epochs above 5 sec.

The minimum discontinuity epoch time for 95% detection probability increases from 10 to 50 second with respect to increasing ω_0.

3.4. Application to real cardio – respiratory data

Results from simulated signals have shown that $\omega_0 = 20$ was optimal when weighing bias, detection error rate and time resolution. Therefore, this value was subsequently used for the analysis of the human data.

(i). Supine rest - Although consistent, the coherence in the HF band is far from being stable, with epochs of weak or no coherence at all (below the threshold level) (Figure 3b). The areas of inconsistency are usually due to a sudden change in breathing and/or in HR (e.g. around 600 and 900 seconds). The epochs of inconsistency may vary in the range of 10 seconds up to 100 seconds.
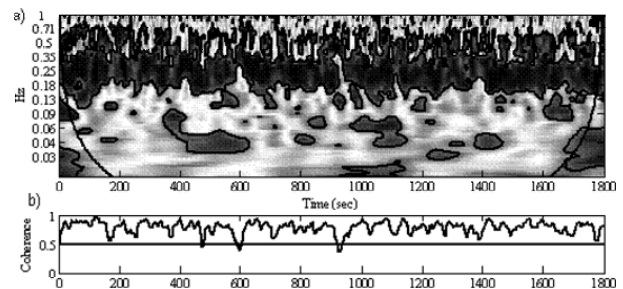

Figure 3: example of typical HR – Resp WTC a) The coherence map. b) The frequency average time dependent coherence of the HF band. The horizontal line is the significance level.
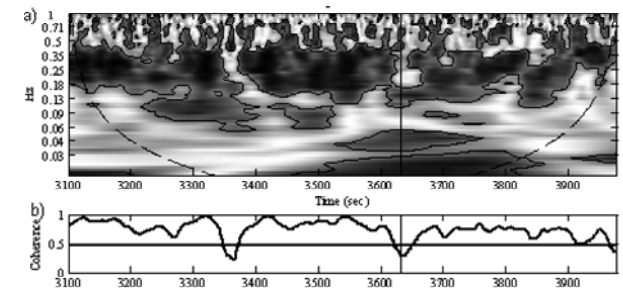

Figure 4: Subject example during CP transition: a) The coherence map. b) time dependent coherence of the HF band. The vertical line marks the onset of the CP. The horizontal line is the significance level.

Not all visible changes in Resp or HR time series give a detectable change in the coherence map or in the HF band averaged coherence.

(ii). Change in Posture (CP) - The band WTC responds with a drop of coherence which reaches its minimum value 20 seconds after CP and recovers to a value significantly lower than in supine position (p<0.001). All subjects experienced a drop beyond the band threshold, which implies a loss of coherence in the HF band. Starting from a value of about 0.75 for supine position, the WTC of HR-RESP stabilizes after the drop at around 0.65 (Figure 4).

4. Discussion and conclusions

We tested the WTC method as a function of the wavelet coefficient ω_0. As expected from spectral analysis [8], the bias and SD increase for smaller ω_0 as well as for lower coherence levels. The small negative bias exhibited on higher coherence level was less expected but has the same magnitude of the SD. The preferred wavelet coefficient to use will be the larger one (above 15), with no major differences between them.

The coherence threshold level acts as a marker for the existence of coupling. Higher threshold values limit the "dynamic range" of the estimates, since only above threshold value is considered as coherence. Therefore, higher ω_0 values are preferable. Error rates are higher for smaller ω_0, again due to the averaging effect of longer (in time) wavelet function and longer smoothing.

The ability to detect transient events and, more specifically, time dependent loss of coherence could be an import advantage in the use of WTC. Smaller ω_0 provided a better ability to detect shorter events.

During supine rest, WTC revealed coherence in the HF band representing RSA, and was consistent overall. Although supine rest is considered as a "steady state" situation, almost all of the subjects exhibited areas of inconsistency in the coupling between the two signals. It can be assumed that most of those below threshold inconsistencies represent real coherence loss.

For all subjects, the CP event caused a general loss of coherence between HR and Respiration. The loss of coherence marks a full system re-adjustment which is evidently a non linear process [10].

The present framework advances WTC as an intuitive and straightforward complementary tool for the bivariate spectral analysis of the ANS regulatory mechanisms. WTC could be applied as a direct tool for the analysis of the dynamic linear coupling between physiological signals, and as a marker for the ANS function. It can also be used for detection of irregularities in the data when a priori assumptions of linear coupling are made.

References

[1] Kay SM. Modern Spectral Estimation: Theory & Application. 1st ed. New Jersey: Prentice Hall; 1988.

[2] Saul JP, Berger RD, Albrecht P, Stein SP, Chen MH, Cohen RJ. Transfer function analysis of the circulation: unique insights into cardiovascular regulation. Am J Physiol Heart Circ Physiol 1991;261(4):H1231-H1245.

[3] Keissar K, Davrath LR, Akselrod S. Time–Frequency Wavelet Transform Coherence of Cardio-Respiratory Signals during Exercise. 2006 p. 733-6.

[4] Cnockaert L, Migeotte PF, Daubigny L, Prisk GK, Grenez F, Sa RC. A method for the analysis of respiratory sinus arrhythmia using continuous wavelet transforms. IEEE Trans Biomed Eng 2008;55:1640-1642.

[5] Ostlund N, Suhr OB, Wiklund U. Wavelet Coherence Detects Non-autonomic Heart Rate Fluctuations in Familial Amyloidotic Polyneuropathy. 2007 p. 4660-2.

[6] Grinsted A, Moore JC, Jevrejeva S. Application of the cross wavelet transform and the wavelet coherence to geophysical time series. Nonlinear Processes in Geophysics 2004;11:561-6.

[7] Torrence C, Compo GP. A Practical Guide to Wavelet Analysis. Bull Am Meteorol Soc 1998;79:61-78.

[8] Bendat SJ, Piersol GA. Random Data: Analysis and Measurement Procedures. New York: Wiley; 1971.

[9] Faes L, Pinna GD, Porta A, Maestri R, Nollo G. Surrogate data analysis for assessing the significance of the coherence function. IEEE Trans Biomed Eng 2004 Jul;51(7):1156-66.

[10] Hainsworth R, Mark AL. Cardiovascular reflex control in health and disease. London: W. B. Saunders Company Ltd; 1993.

Address for correspondence

Kobi Keissar
Abramson Center for Medical Physics, Sakler Faculty of Exact Sciences, Tel Aviv University
Tel Aviv, Israel 69978
keissar@post.tau.ac.il